

# Numerical Study of Flow Separation Control over a NACA2415 Airfoil

M. Tahar Bouzaher

**Abstract**—This study involves numerical simulation of the flow around a NACA2415 airfoil, with a  $18^\circ$  angle of attack, and flow separation control using a rod. It involves putting a cylindrical rod -upstream of the leading edge- in vertical translation movement in order to accelerate the transition of the boundary layer by interaction between the rod wake and the boundary layer. The viscous, non-stationary flow is simulated using ANSYS FLUENT 13. The rod movement is reproduced using the dynamic mesh technique and an in-house developed UDF (User Define Function). The frequency varies from 75 to 450 Hz and the considered amplitudes are 2%, and 3% of the foil chord. The frequency chosen closed to the frequency of separation. Our results showed a substantial modification in the flow behavior and a maximum drag reduction of 61%.

**Keywords**—CFD, Flow separation, Active control, Boundary layer, rod, NACA 2415.

## I. INTRODUCTION

THE need to understand low Reynolds number aerodynamics has gained more attention due to variety of mechanical applications as Unmanned Air Vehicle (UAV), Micro Air Vehicle (MAV) and wind turbine. [1] The presence of laminar separation bubble has a deteriorating effect on the performance of this device. The understanding of the physics of this bubble and the possible ways to control it thus are essential prerequisites for efficient design of these systems M. Serdar Genç et al. [1] studied the boundary layer separation on a NACA2415 airfoil using hot-wire anemometry and oil flow visualization method, to photograph the surface flow patterns. The experimental results showed that when the angle of attack increased, the separation and the transition points move towards the leading edge. Mittal et al. [2] characterized the different frequencies scales present in a separated flow to understand the physical of the separation control by steady and pulsed vortex Generator Jets. The review of Greenblatt et al. [3] summarized the flow separation control by periodic excitation in various forms. Flow control through boundary layer can reduce the drag, enhance the lift, and improve the performance of the aircraft. Among the used methods, vortex generators (VG) have been widely used. Igarashi et al. [4] use a rod as vortex generators to control the flow around a square cylinder for a Reynolds number of  $3.2 \times 10^4$ , a drag reduction of 50% was registered with taking into account the drag of the cylindrical rod. The experimental study of Igarashi et al. [5] on the effect of the interaction between the wake of a cylindrical rod, and the boundary layer of a vertical disc

indicated a drag reduction between 20% and 30% compared to the case without cylindrical rod. Tsutsui et al. [6] set the cylindrical rod to a circular cylinder in order to reduce drag force; they have found with the ratio  $d/D = 0.25$  a drag reduction about (63%) where  $d$  and  $D$  present respectively the rod and the cylinder diameter. The aim of this work is to study the flow separation control using a rod-airfoil configuration. The study focuses on estimating the characteristic aerodynamics and the efficiency of this strategy in drag reduction.

## II. MOTION MODELING AND DEFORMABLE MESH

We divided the calculation domain into three zones (Fig. 1). This allows keeping the same mesh throughout simulations in the close area surrounding the rod. Zone 1 contains the rod, it is meshed with a quadrilateral structured grid, and this zone simulates the vertical sinusoidal motion. Zone 2 consists of a structured quadrilateral grid and divided into two parts, which are located above and below Zone 1. The height of each of Zone 2 parts changes during the calculations

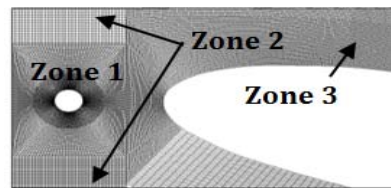


Fig. 1 Rod-foil geometrical characteristics

The rod movement is governed by the following law

$$h = h_0 c \cos(2\pi f t)$$

where  $h$  is the instantaneous airfoil position along the y axis,  $h_0$  the maximal amplitude of the movement,  $c$  the airfoil chord,  $f$  the frequency, and  $t$  the time. The total drag and lift coefficients are defined, respectively, as:

$$C_{DT}(t) = C_{DFoil} + C_{DRod} = \frac{F_{1X}(t)}{\left(\frac{1}{2}\right)\rho(U(t))^2 C \sin\alpha} + \frac{F_{2X}(t)}{(1/2)\rho(U(t))^2 d}$$

$$C_{LT}(t) = C_{LFoil} + C_{LRod} = \frac{F_{1Y}(t)}{\left(\frac{1}{2}\right)\rho(U(t))^2 C \cos\alpha} + \frac{F_{2Y}(t)}{(1/2)\rho(U(t))^2 d}$$

where,  $F_{1X}(t)$  and  $F_{2X}(t)$  represent, respectively, the instantaneous total force in the x-direction (longitudinal) apply in the foil and in the rod,  $F_{1Y}(t)$  and  $F_{2Y}(t)$  represent, respectively, the instantaneous total force in the normal

M. T. Bouzaher is a Research Associate at the Department of Mechanical Engineering of the University of Biskra, 07000, Algeria (e-mail: mohamedbouzaher@yahoo.fr).

(transversal) direction apply in the foil and in the rod,  $t$ , the time,  $c$  the airfoil chord, and  $d$  the diameter rod.

The period-averaged consumption power and consumption power rate can be evaluated respectively, as:

$$P = \int_{t_n}^{t_n+1/f} F_y(t) \frac{dh}{dt} dt,$$

$$C_p = \frac{f \int_{t_n}^{t_n+1/f} F_y(t) \frac{dh}{dt} dt}{(1/2)\rho(U)^3 d}$$

where  $dh/dt$ , is the traveling velocity of the vertical motion,  $U$  is the imposed velocity, and  $[t_n, (t_n + 1/f)]$  is the last period of the movement.

#### A. Mesh Independence

To study the simulation results mesh independent, many cases were simulated with several mesh concentrations. The drag (lift) evolution in function of cells number was given in Figs. 3 and 4. The number of cells used in all cases was between 0.2 and 0.3 million. Generally, we require a larger number of cells to realize mesh which is able to give a good estimation of aerodynamics forces and flow characteristics. The pressure distributions over the foil surface for the natural case (without a rod) were also compared with those given by Serdar Genç [1]. The maximum error was about 3%. The results show a good agreement between this study and the previous works (Fig. 2).

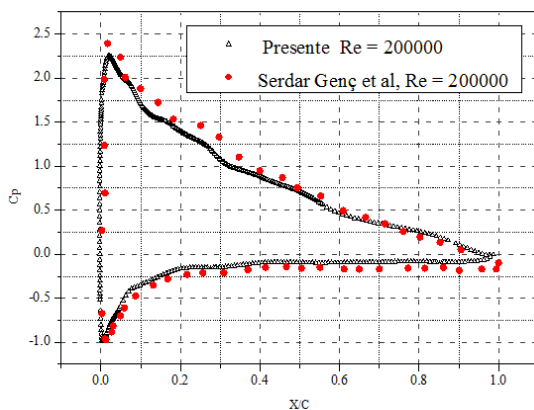


Fig. 2 Pressure coefficient

### III. DRAG AND LIFT COEFFICIENTS

The time history of lift and drag coefficients plotted in Fig. 5 show that the lift and the drag oscillate in time with a quasi-sinusoidal way. These oscillations are due to the periodic vortex shedding mechanism. Figs. 6 and 7 indicate a decrease in the total lift coefficient and an increase in that of drag. For an amplitude of 2%  $c$  at the frequency 75HZ the drag coefficient is near to that of the case without control and this is essentially due to the weak interaction between the rod wake and the leading edge vortices, also to the formation of large structures which develop along the upper surface (Fig. 11).

For the amplitude of 3%  $c$  we note a pronounced reduction in the drag coefficient in the range  $1 \leq fc/fn \leq 2.5$ . The rod lift force oscillates in a stable quasi-periodic mode around zero and the drag around one, the lift magnitude is approximately twice of drag. The plots of consumption power versus moving frequency (Fig. 8) show an exponential behavior, we noted that the consumption power increases with the frequency increases this is essentially due to the fact that the rod velocity increases with frequency increases.

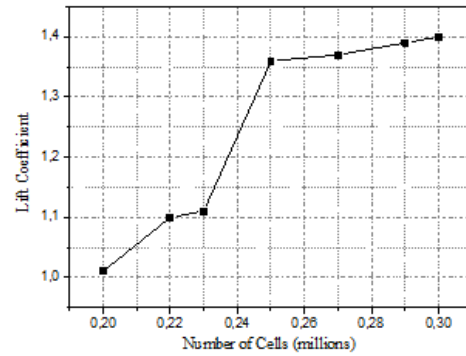


Fig. 3 Lift coefficient versus number of mesh volumes

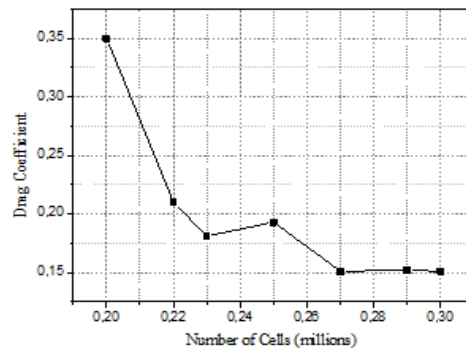


Fig. 4 Drag coefficient versus number of mesh volumes

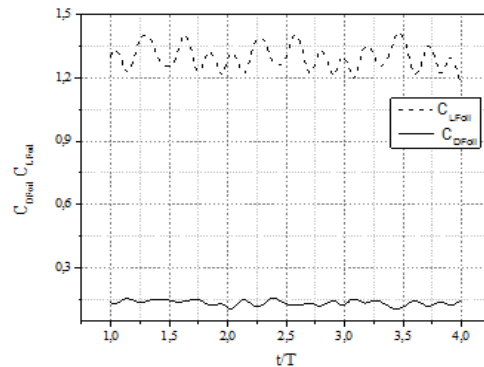


Fig. 5 Time history of lift and drag coefficients

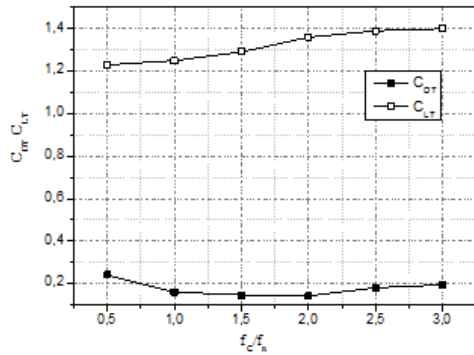


Fig. 6 Time-averaged total lift and drag coefficient  
For an amplitudes 2% c

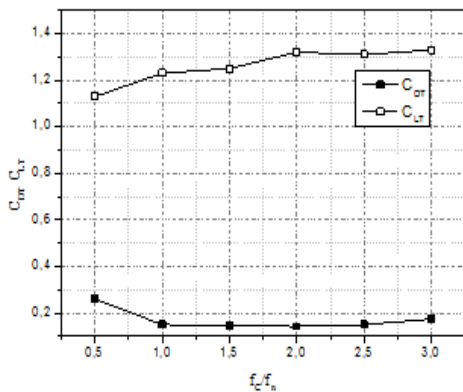


Fig. 7 Time-averaged total lift and drag coefficient  
For an amplitudes 3% c

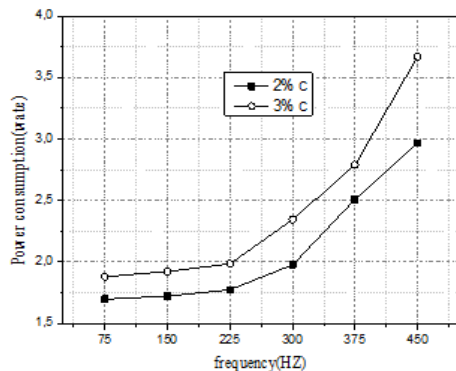


Fig. 8 Period averaged consumption power

Let us note that the natural shedding frequency  $fn = 150\text{Hz}$  corresponds to the periodic shedding of large structures (foil) with a wake mode of thick bodies. The mean pressure coefficient  $C_p$  of the foil in the case without control present an isobar plateau corresponds to the separation bubble (Fig. 9). The skin friction coefficient  $C_f$ , on the upper surface of the airfoil is shown in Fig. 9. The negative value of  $C_f$  shows the near-wall reversed flow in the separation bubble. The  $C_f$  values for the case without control indicates that the separation starts at  $x = 0.05C$  near the leading edge. The

separated flow reattaches near  $x = 0.21C$ . The average length of the separation bubble is about  $0.15C$ . The  $C_f$  values for all cases with control show a significantly reducing or a total elimination of the laminar separation bubble.

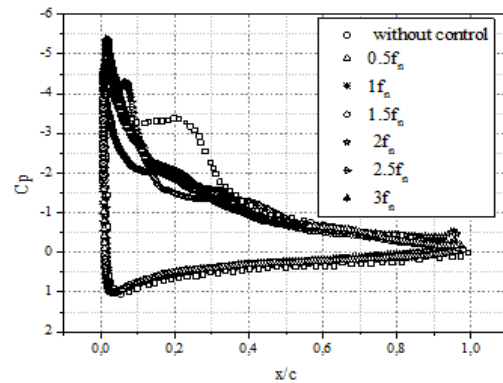


Fig. 9 Mean pressure coefficient

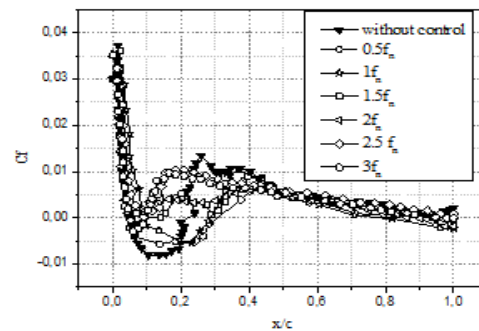


Fig. 10 Mean skin friction coefficient

The mean pressure coefficient curves show an increase in depression at the leading edge results in an increase in the lift coefficient. The best performances for the drag reduction are for a frequency equal to the double of the natural frequency with a value of 60%. In this case, the lift is not the largest this one is marked for a frequency equal to the natural frequency with a value of 35%. One notes that the location and length of the separation bubble are changed under the control effect.

#### IV. FLOW VISUALIZATION

The instantaneous fields of vorticity which show creation, the development and detachment of the flow vortices for a one-period ( $T$ ), are given on Fig. 10. It was noted that the zone of recirculation does not exist at the leading edge; in fact, the wake of the rod interacts with the separated zone, and allowing the formation of small structures along the upper surface. We remarked, also, the presence of the Kelvin-Helmholtz waves which occur starting from the trailing edge. These waves are vortices which appear when the velocity profile presents a point of inflection and is characterized by a strong amplification rate. The difference in velocity between the under and the upper surface of the foil induces also a shearing in the mixture layer. It is also noted that small

vortices developed on the under-surface, in fact when the rod is moving the upper surface of the foil which is a zone of low pressure cannot aspire all fluid particles created by the rod.

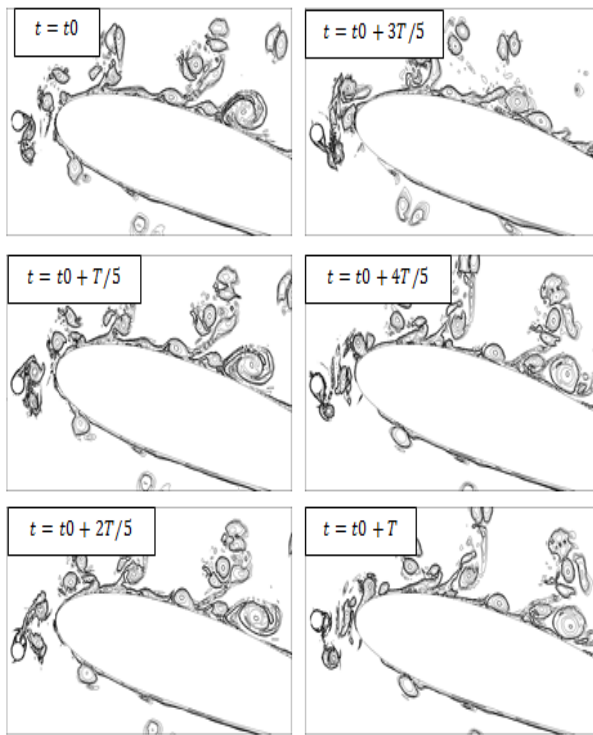


Fig. 11 Vorticity field for the case “2.5Fn”.

#### V.CONCLUSION

In this study we considered the effect induced by the presence of a moving rod in the aerodynamics coefficients and flow structure. We noted a total modification in the flow behavior. Our results show that the laminar separation bubble disappears completely for the optimal case and a maximum drag reduction of 61% was registered.

#### REFERENCES

- [1] Serdar Genc, M., Hakan, k Acikel, H. An experimental study on aerodynamics of NACA2415 aerofoil at low Re numbers Journal of Experimental Thermal and Fluid Science: 10.1016.
- [2] Mittal R., Kotapati R.B. et Cattafesta L. 2005. "Numerical study of resonant interactions and flow control in a canonical separated flow". AIAA Paper, No. 2005-1261.
- [3] Greenblatt D, Wygnanski IJ. The control of flow separation by periodic excitation. Prog Aerospace Sci 2000;36:487–545.
- [4] Amotsu Igarashi. (1997) "Drag reduction of a square prism by flow control using a small rod". Journal of Wind Engineering and Industrial Aerodynamics; 69 71 141-153.
- [5] Igarashi, T., Nobuaki, T. Drag reduction of flat plate normal to airstream by flow control using a rod. Journal of Wind Engineering and Industrial Aerodynamics 90 (2002) 359–376.
- [6] T.sutsui, Igarashi, T. Drag reduction of a circular cylinder in an air-stream Journal of Wind Engineering and Industrial Aerodynamics 90 (2002) 527–541.